Acta Radiologica Short Reports
4(1) 1–15

DOI: 10.1177/2047981614562443
arr.sagepub.com
SAGE

# Imaging pitfalls, normal anatomy, and anatomical variants that can simulate disease on cardiac imaging as demonstrated on multidetector computed tomography

**Silanath Terpenning[1] and Charles S White[2]**

## Abstract

Advances in computed tomography have led to continuous improvement in cardiac imaging. Dedicated postprocessing capabilities, faster scan times, and cardiac gating methods reveal details of normal cardiac anatomy and anatomic variants that can mimic pathologic conditions. This article will review normal cardiac anatomy and variants that can mimic disease. Radiologists should be familiar with normal cardiac anatomy and anatomic variants to avoid misinterpretation of normal findings for pathologic processes.

**Keywords**

Cardiac computed tomography (CT), cardiac CT anatomy, cardiac anatomy, anatomical variants, imaging pitfalls

Date received: 18 July 2014; accepted: 10 November 2014

## Introduction

Substantial advances in multidetector computed tomography (CT) scans, hardware, software, and postprocessing capability have led to marked improvement in the display of cardiac anatomy and pathology. The use of CT scanners with 64 or more detectors is now standard and ECG-gating capabilities are widely available. In this article, we review normal cardiac anatomy and commonly encountered pitfalls using a chamber-specific approach.

## Technique

Current CT scanners produce temporal resolution below 250 ms and in some instances less than 100 ms. Although this permits adequate assessment of cardiac structures during conventional CT acquisitions, ECG-gating should be used to optimize imaging and reduce the potential for artifacts that may lead to misinterpretation. The use of beta-blockers to reduce rapid heart rates and couching for breath-holding are important adjunctive strategies to reduce artifacts.

For most anatomic questions, prospective ECG-gating that provides a snapshot image of the heart during a small part of the cardiac cycle is sufficient and allows radiation sparing. If functional information is required, retrospective ECG-gating acquired throughout the cardiac cycle is necessary. Delayed imaging may also be useful in certain circumstances.

Reformatted images are often a critical part of evaluation of cardiac structures. Multiplanar images can be reconstructed in specific cardiac planes to highlight normal anatomy and variants. Maximum intensity projection and volumetric images may provide additional perspective that may be valuable to the interpreting and referring physicians.

[1]Department of Radiology, University of New Mexico, Albuquerque, NM, USA
[2]Department of Radiology, University of Maryland, Baltimore, MD, USA

**Corresponding author:**
Silanath Terpenning, Department of Radiology, University of New Mexico, MSC 10 5530, 1 University of New Mexico, Albuquerque, NM 87131, USA.
Email: natsawadee@yahoo.com

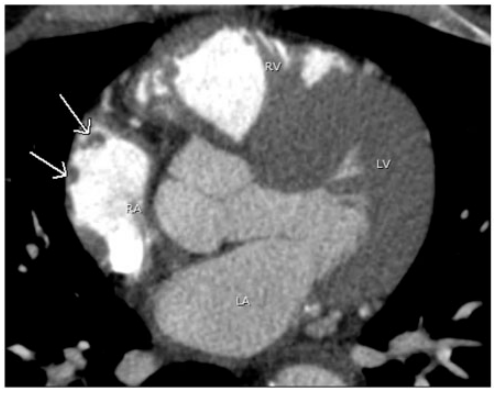


**Fig. 1.** A 44-year-old man with atrial fibrillation. A pulmonary vein CT for pre-ablation mapping shows multiple small filling defects abutting the lateral wall of the right atrium (arrows), compatible with prominent pectinate muscles. Note contrast opacification in the right heart due to poor timing. LA, left atrium; LV, left ventricle; RA, right atrium; RV, right ventricle.

## Cardiac anatomy and variants

### *Right atrium*

The right atrium develops from the primitive right atrium and sinus venosus. The sinus venosus forms a smooth wall called the sinus venarum and receives blood from the inferior vena cava, superior vena cava, and coronary sinus. The primitive right atrium forms the trabeculated aspect of the right atrial appendage. The right atrial appendage has a triangular or pyramidal shape with a wide base opening and rough trabeculation of the pectinate muscles (1,2). The pectinate muscles in the RAA may be misinterpreted as a mass or thrombus (Fig. 1). Careful observation of the parallel course of the pectinate musclature to the wall of right atrium on axial or reformatted images will confirm this normal structure (3).

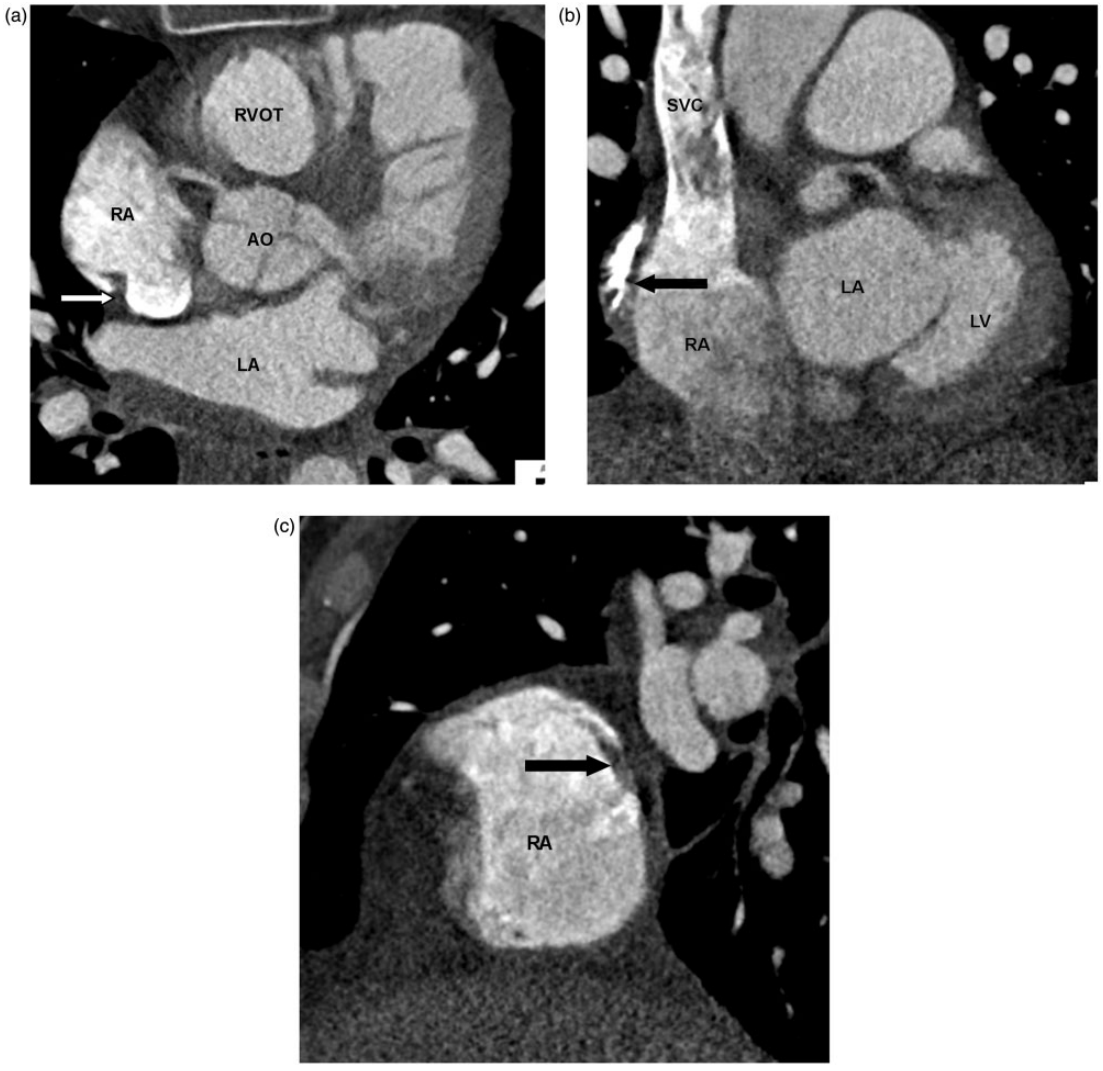


**Fig. 2.** A 62-year-old man with chest pain and prior myocardial infarction. Multiplanar images of a coronary CTA for coronary artery evaluation show the normal crista terminalis identified as a smooth soft tissue ridge along the posterolateral wall of right atrium on axial (white arrow in a), coronal and sagittal planes (black arrow in b, c). AO, aorta; RVOT, right ventricular outflow tract; SVC, superior vena cava.

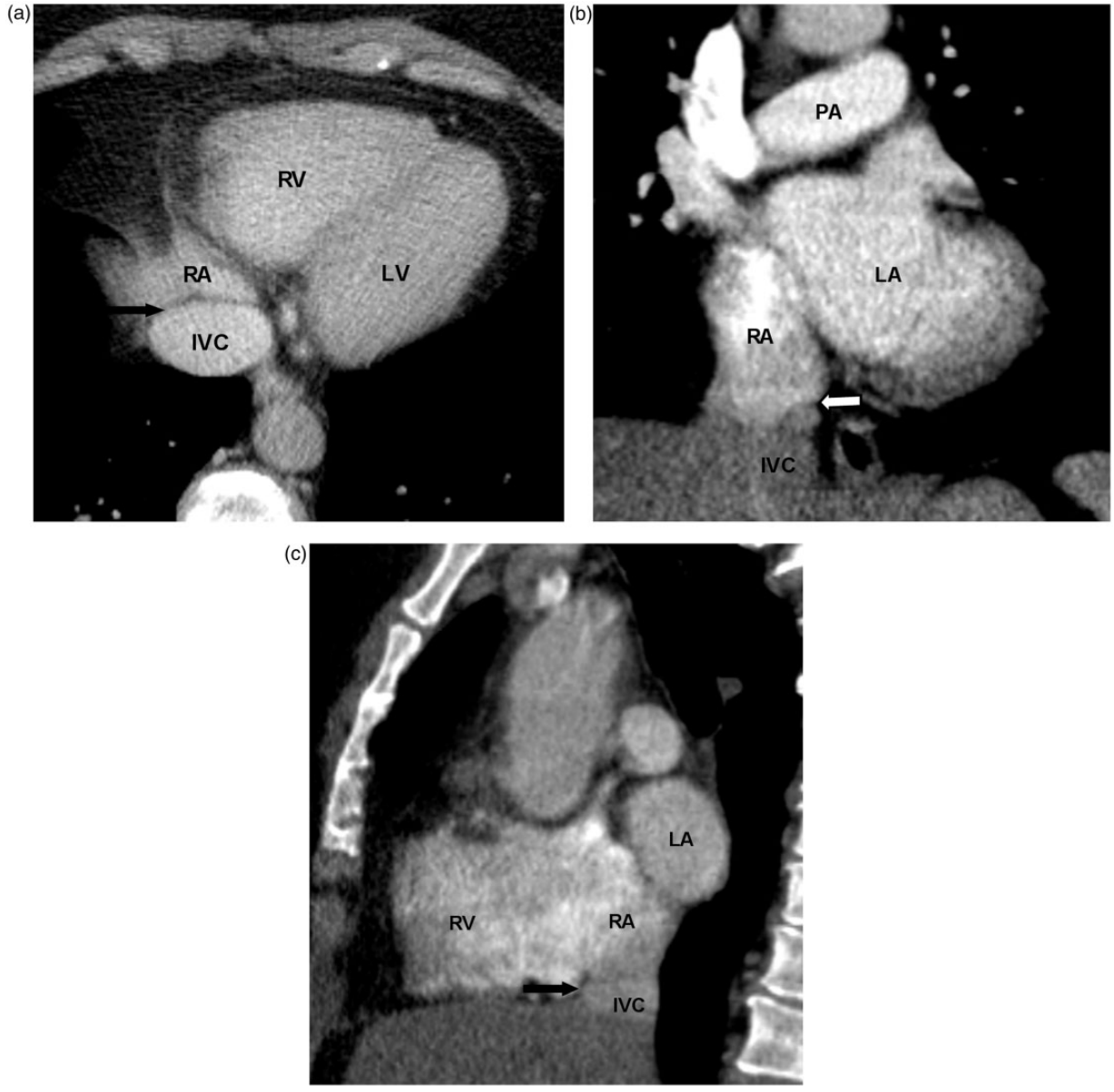


**Fig. 3.** A 61-year-old woman with head and neck cancer. Chest CT with contrast was performed for restaging. Normal Eustachian valve is seen as a paper-thin structure at the junction of IVC and RA on axial (black arrow in a), coronal (white arrow in b), and sagittal planes (black arrow in c). IVC, inferior vena cava; PA, pulmonary artery.

The crista terminalis is a vertically orientated smooth muscle ridge extending from the superior vena cava to the inferior vena cava. It represents the fusion line between the primitive RA and the posterior smooth wall of the sinus venosus portion of the right atrium (1). Some authors believe that there is an internodal conductive pathway between the sinoatrial and atrioventricular nodes within the crista terminalis, which traverses the Eustachian region, and enters the atrioventricular node posteriorly via the coronary sinus (4). Since the size and shape of the crista terminalis can be variable, it may be mistaken for an intracardiac mass or thrombus (3,5–8) (Fig. 2a–c).

The Eustachian valve is located at the junction of the inferior vena cava and right atrium. This valve is associated with a Chiari network, which is a collection of fibrous structures. The Eustachian valve is commonly seen on MRI (2), less often appreciated on CT due to the inflow of unopacified blood from the inferior vena cava (9). The Eustachian valve directs blood flow towards the foramen ovale and normally regresses during embryonic development. It is typically a thin and mobile structure (2) (Fig. 3).

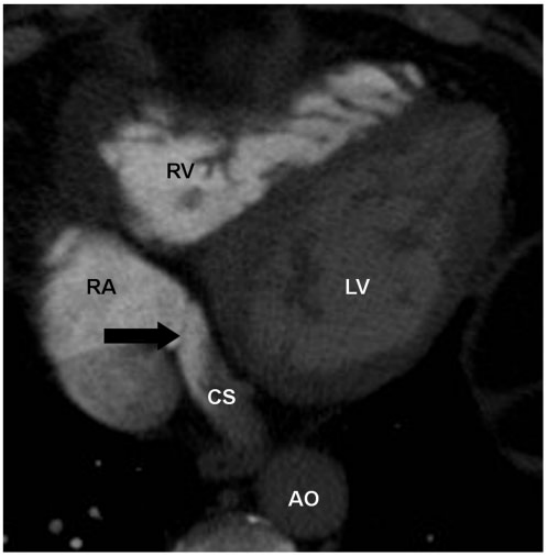


**Fig. 4.** A 66-year-old man with chest pain. CTA of the chest performed to rule out pulmonary embolus shows an incompetent Thebesian valve (arrow). CS, coronary sinus.

The Thebesian valve is located within the right atrium at the orifice of the coronary sinus. It prevents reflux of blood from the right atrium into the coronary sinus (10) (Fig. 4). Both of these valvular structures can be variable in size, shape, and appearance and should not be mistaken for neoplasm, thrombus, or inflammation (11).

## *Left atrium*

The left atrium is the most posterosuperior chamber and receives pulmonary venous return. It is attached to the left atrial appendage. The primitive left atrium forms a single pulmonary vein which later divides into four pulmonary veins. The posterior wall of the primitive left atrium, which normally receives the four pulmonary veins, becomes the smooth portion of the left atrium proper. The remainder of the primitive left atrium becomes the trabeculated portion or left atrial appendage (1) (Fig. 5).

Compared to the right atrial appendage, the left atrial appendage is more tubular in shape, has a narrower base, and contains fewer trabeculated pectinate muscles (2). The pectinate muscles can have a linear or globular appearance and can be misinterpreted as an intracardiac mass or thrombus (12) (Fig. 6). This issue can be resolved by close observation of the course of the pectinate muscles, which are parallel in configuration. In contrast, thrombus is seen as a focal filling defect. If doubt exists, reformatted images will confirm the diagnosis (3).

Blood flow in the left atrial appendage is sluggish and therefore prone to thrombus formation (Fig. 7a, b). The presence of thrombus may alter patient management, particularly if left atrial appendage closure devices are being considered. Dependent contrast and unopacified blood causing a contrast-fluid level in the left atrium can lead to the unopacified component being confused with thrombus (3). Repeat CT with delayed scanning in the venous phase (approximately 30 s later) at the same level will show a well opacified left atrial appendage although echocardiography may be necessary for clarification. Thrombus in the left atrium and left atrial appendage is often associated with atrial fibrillation or cardiac chamber and valvular abnormalities (13).

The left atrial oblique vein is an embryologic remnant of the left superior caval vein. The left superior caval vein is enclosed within the Marshall ligament, which is a fold of the visceral pericardium containing muscle, vascular, and nervous structures (14,15). The ligament of Marshall courses obliquely above the left atrial appendage and lies laterally to the left superior pulmonary vein bundle in the epicardial aspect of the left atrial fold, forming the left posterior crest (16). It is also known as the Coumadin or Warfarin ridge, or Q-tip. This can be mistaken as a pedunculated mass or thrombus (17). Historically, this structure was misinterpreted as a thrombus on echocardiography, resulting in anticoagulation therapy with Warfarin. The Q-tip name derives from an appearance on echocardiography that simulates a Q-tip. This normal structure is well visualized on multiplanar rendering (MPR) imaging (Fig. 8a–c).

The interatrial septum is thin and often not well visualized on imaging studies. Normal fat deposition within the septum measures between 0.9–9.9 mm in thickness (18). Due to advanced age or obesity, increased fat deposition occurs and makes the septum easier to visualize. The most common abnormality of the interatrial septum is lipomatous hypertrophy of the interatrial septum, defined as fatty deposition within the interatrial septum of more than 2 cm in thickness that spares the fossa ovalis (19). This is present in up to 2.2% of patients and is occasionally associated with pulmonary emphysema and atrial arrhythmia (20). The characteristic features include a smoothly marginated, non-enhancing dumbbell-shaped fatty mass sparing the fossa ovalis (18–20) (Fig. 9).

Embryologic development of the interatrial septum includes normal thinning of the septum at the fossa ovalis (Fig. 10). This physiologic thinning at the fossa ovalis can simulate an atrial septal defect (21). Lack of flow between the left atrium and the right atrium on dynamic studies in the region of the thinned septum confirms this normal appearance. If the findings are equivocal, echocardiography or MRI can be used for further evaluation.

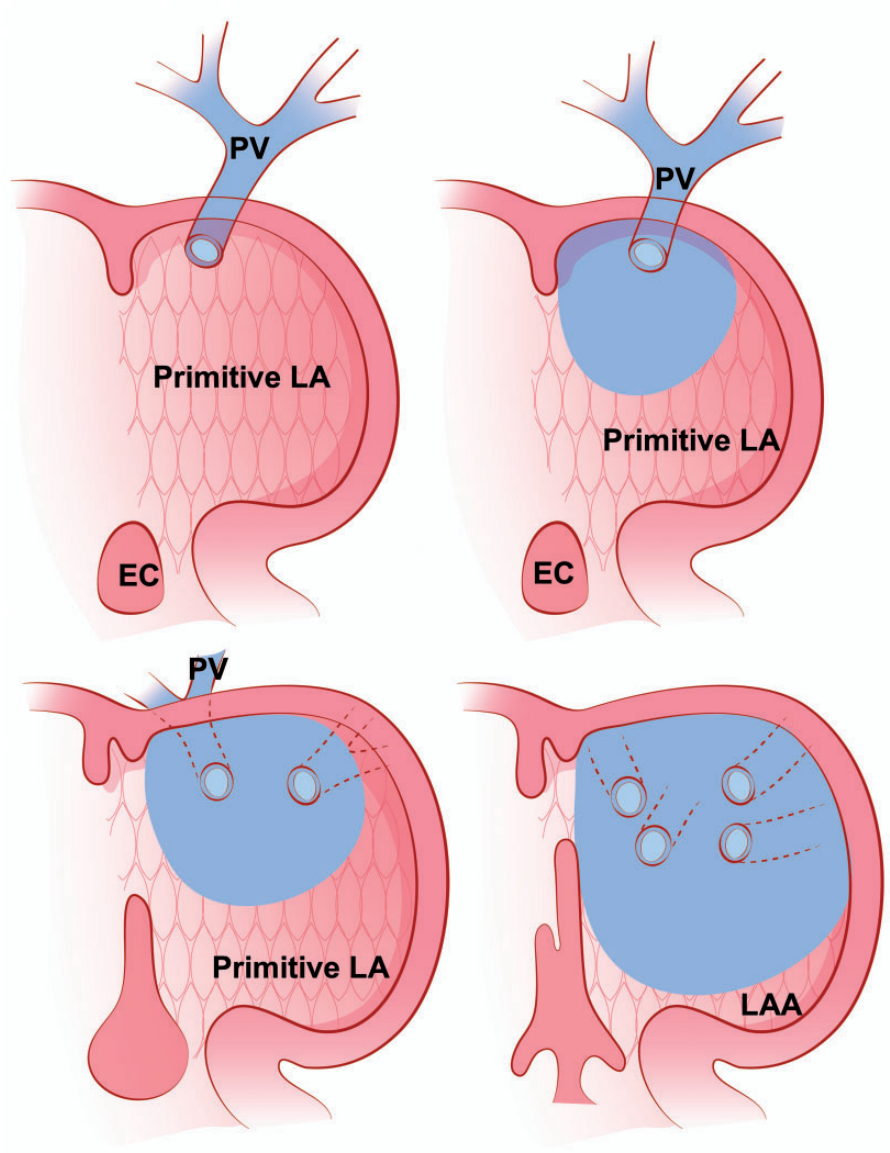


**Fig. 5.** An illustration shows the embryologic development of the left atrium. A primitive pulmonary vein opens into the primitive left atrium then the pulmonary vein divides into four pulmonary veins. A part of the pulmonary vein becomes a smooth-walled part of the left atrium (blue). The primitive left atrium (the trabeculated part with patterned pink background) becomes left atrial appendage. EC, endocardial cushion; LA, left atrium; LAA, left atrial appendage; PV, pulmonary vein. This illustration was modified with permission from: Moore KL, Persaud TVN. The Developing Human: Clincially Orientated Embryology. 8th edition. Amsterdam: Elsevier, 2008:303.

Seventy-five percent of septum primum and septum secundum tissues fuse after birth. If the foramen ovale (FO) is covered but does not completely seal, it results in a patent foramen ovale (PFO). A PFO is a persistent valvular-like connection between the RA and LA, which usually results in a left to right shunt (Fig. 11). Although most patients with PFO are asymptomatic, they may suffer from desaturated blood and embolic events (22,23).

### *Right ventricle*

The right ventricle is located in the most anterior portion of the heart. It has a complex triangular shape and receives blood from the right atrium. It is more trabeculated and thinner than the left ventricle. The unique features of the right ventricle include heavy trabeculation and the presence of the moderator band (2,10).

The right ventricle contains three components: (i) the inlet consisting of the tricuspid valve, chordae tendinae, and papillary muscles; (ii) the trabeculated apical myocardium; and (iii) the infundibulum, or conus, which corresponds to the smooth outflow tract (24). The landmarks separating the right ventricle inlet and outlet are variably reported to be septomarginal trabeculation (25) or the infundibuloventricular fold (26).

In the embryologic period, the fetal heart forms trabecule carneae, numerous muscle bundles running in the ventricles and locating on the inner ventricular surfaces. During embryonic development, division of cardiomyocytes leads to formation of typical trabeculae (27).

The prominent muscular bands within the right ventricle are composed of the parietal band, septomarginal band, septal band, and moderator band (28,29).

The most commonly seen septomarginal trabeculation is the moderator band, a heavily trabeculated muscle and a unique feature of the right ventricle (Fig. 12). It is a tissue ridge that extends across the right ventricular apex from the anterior papillary muscle to the interventricular septum. It contains the right bundle branch (2,10). The displaced moderator band can simulate a double-chambered right ventricle (30) and a prominent moderator band in right ventricular enlargement or hypertrophy can be mistaken for thrombus or tumor (31).

The right ventricle contains three papillary muscles: the anterior, posterior, and medial papillary muscles. Each muscle attaches to two cusps (2,32). The most commonly seen muscle is the anterior papillary muscle (Fig. 13a–c). If prominent, this structure can be mistaken for an intracardiac mass or thrombus.

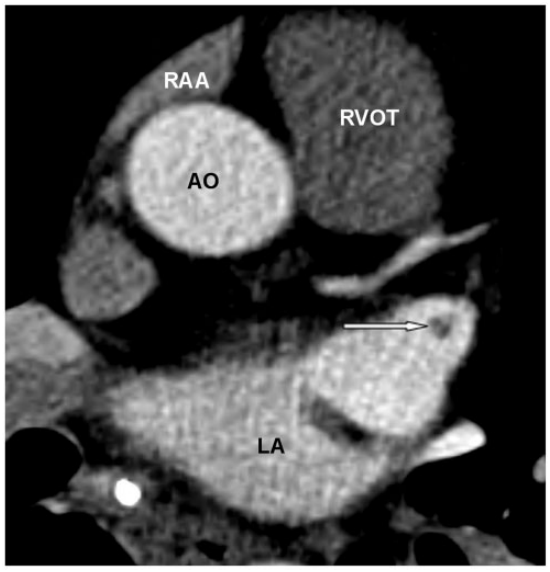


**Fig. 6.** A 42-year-old woman with atrial fibrillation. A pulmonary vein CT for pre-ablation mapping shows a filling defect in the left atrial appendage. Its course on the dynamic images appears to be a pectinate muscle (arrow). RAA, right atrial appendage.

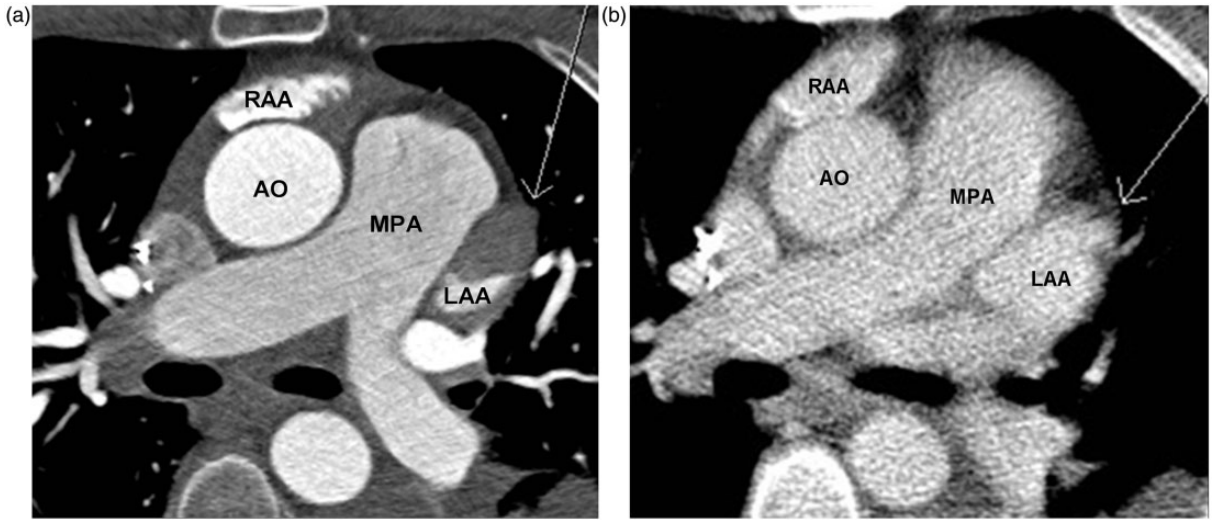


**Fig. 7.** A 79-year-old woman with atrial fibrillation. CT of the pulmonary vein prior to left atrial appendage ligation showed a filling defect in the left atrial appendage (arrow in Fig. 7a) which was filled in on the delayed image (arrow in Fig. 7b). This is sluggish flow in the left atrial appendage simulating left atrial appendage thrombus. LAA, left atrial appendage; MPA, main pulmonary artery.

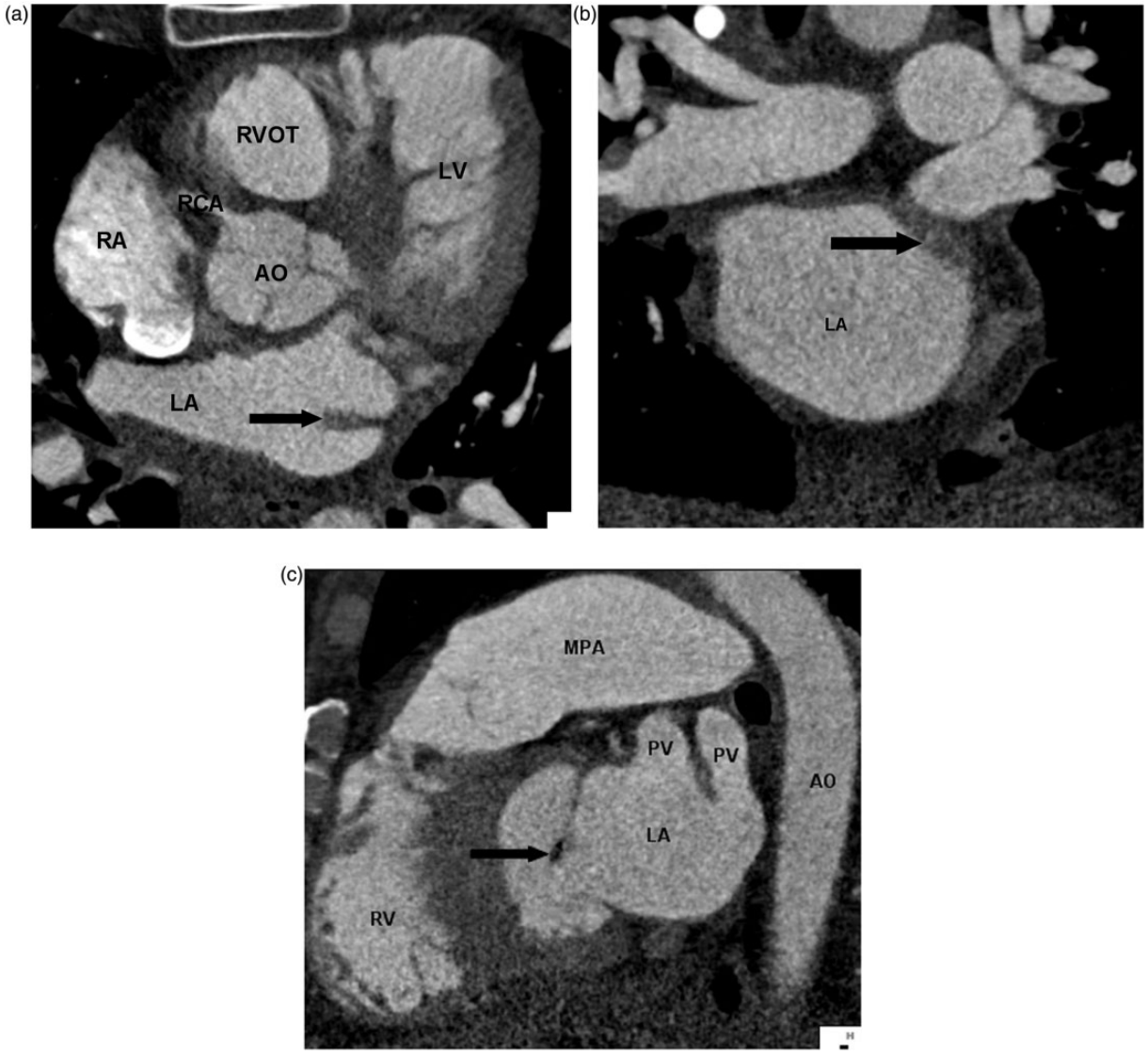


**Fig. 8.** A 62-year-old man with chest pain. Coronary CTA was performed to evaluate coronary artery. On axial (a), and multiplanar reformatted coronal (b) and sagittal (c) planes, the Ligament of Marshall, an embryonic remnant at the junction of left superior pulmonary vein and left atrium is seen as a smooth tissue ridge (black arrow). PV, pulmonary vein; RCA, right coronary artery.

If doubt persists, reformatted images will confirm the diagnosis (3).

Non-specific fat deposition in the right ventricle is found in up to 17% of asymptomatic subjects and is most often encountered in the elderly. Common locations are the superior wall of the base, the middle segment of the right ventricle, and the right ventricular outflow tract. Fat deposition can mimic arrhythmogenic right ventricular dysplasia or prior myocardial infarction involving the right ventricle (33) (Fig. 14). Functional assessment can be used to differentiate variants from a diseased right ventricle.

## *Left ventricle*

The left ventricle consists of the inlet, apical, and outlet portions and is separated from right ventricle by the interventricular septum. The septum typically bulges toward the right ventricle due to pressure differences between the chambers (2).

The left ventricle contains two papillary muscles, the anterior and posterior papillary muscles, which are larger than the papillary muscles of the right ventricle. Chordae tendinae attach the papillary muscles to the mitral valve leaflets (2). The posterior papillary muscle

can have a globular shape and can be misinterpreted as a mass or thrombus (3). Two unique features of the left ventricle are a smooth wall and shared annulus between the mitral and aortic valves. Both anterior and posterior papillary muscles are well appreciated on MPR images (Fig. 15a–c).

In a minority of the population, false tendons or false chordae occur as normal variants in the left ventricle. These false chordae are linear structures attached at both ends to the endomyocardium (34). They are asymptomatic and usually incidental findings on echocardiography (31).

The normal wall thickness of the left ventricular myocardium is 6–11 mm. Focal wall thinning at the apex with normal cardiac function in the absence of symptoms or history of myocardial infarction is

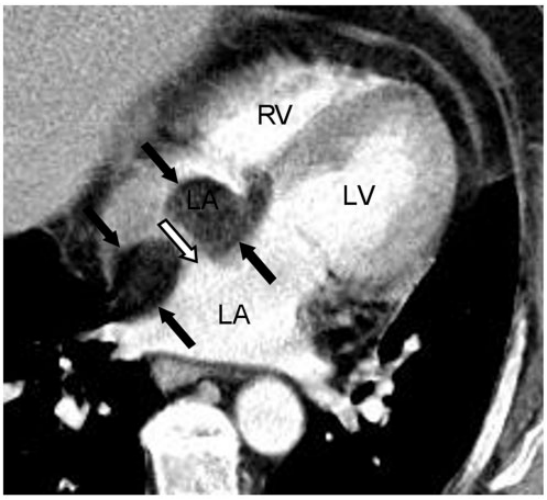


**Fig. 9.** A 64-year-old man with history of lung nodule. A chest CT performed for re-evaluation of the nodule shows lipomatous hypertrophy of the interatrial septum (black arrows). The typical radiographic findings include a dumbbell-shaped fatty mass and sparing of the fossa ovalis (white arrow).

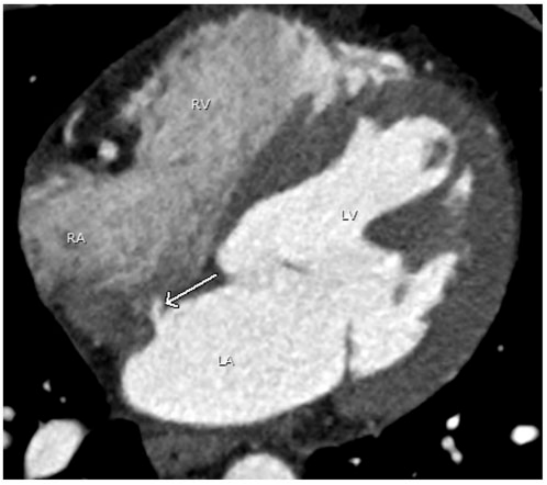


**Fig. 11.** A 37-year-old man with atypical chest pain. Coronary CTA performed to rule out coronary artery disease shows a small jet of contrast from left atrium to right atrium, compatible with patent foramen ovale (arrow). This is more conspicuous on the dynamic study. No coronary artery disease was found.

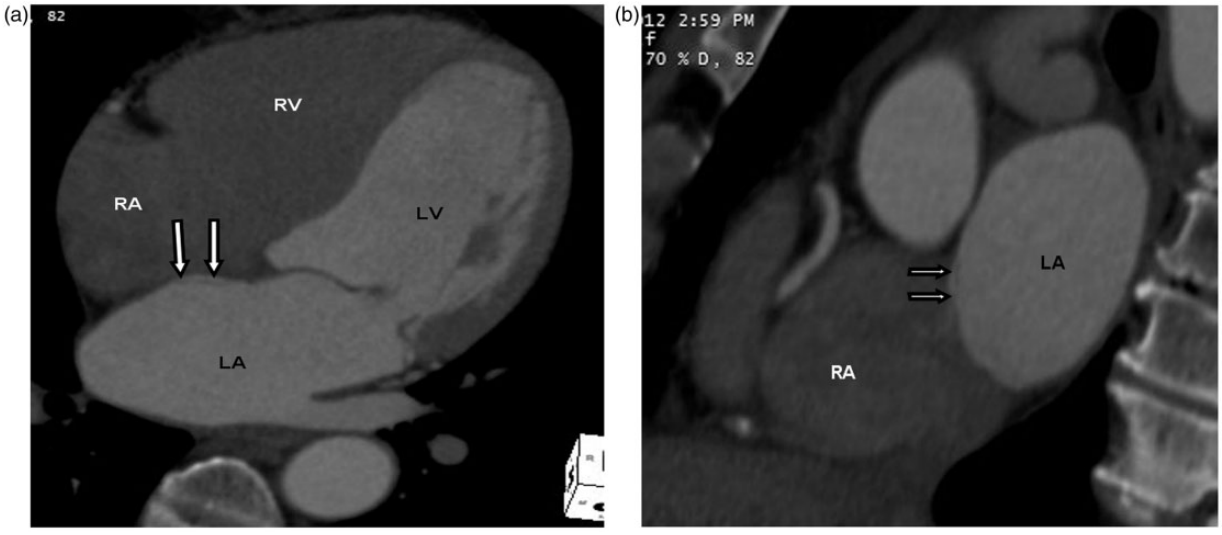


**Fig. 10.** A 74-year-old woman with left ventricular thrombus seen on echocardiogram. Cardiac CT was performed to rule out left ventricular thrombus. The normal thinning of interatrial septum at the fossa ovalis is seen adjacent to the left atrial pouch, corresponding to the unfused septum primum and secundum on four chamber (double white arrows in a) and sagittal oblique views (double white arrows in b). This can be mistaken for an atrial septal defect.

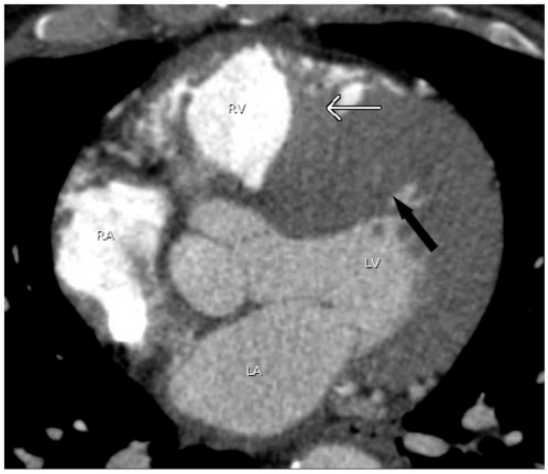


**Fig. 12.** A 45-year-old man with chest pain. A chest CTA performed to rule out pulmonary embolism shows a prominent moderator band (white arrow) running between the RV free wall and interventricular septum (black arrow).

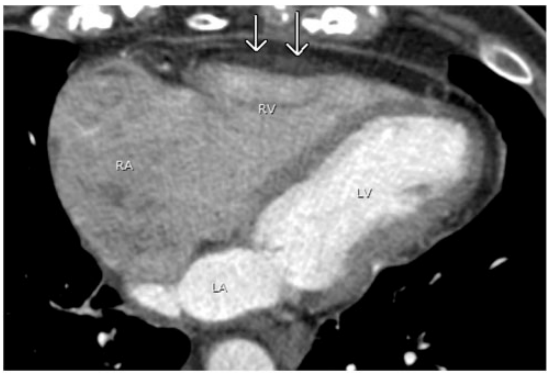


**Fig. 14.** A 63-year-old woman with atrial fibrillation. A pulmonary vein CT for pre-ablation mapping shows nonspecific fat deposition in the RV free wall (double arrows).

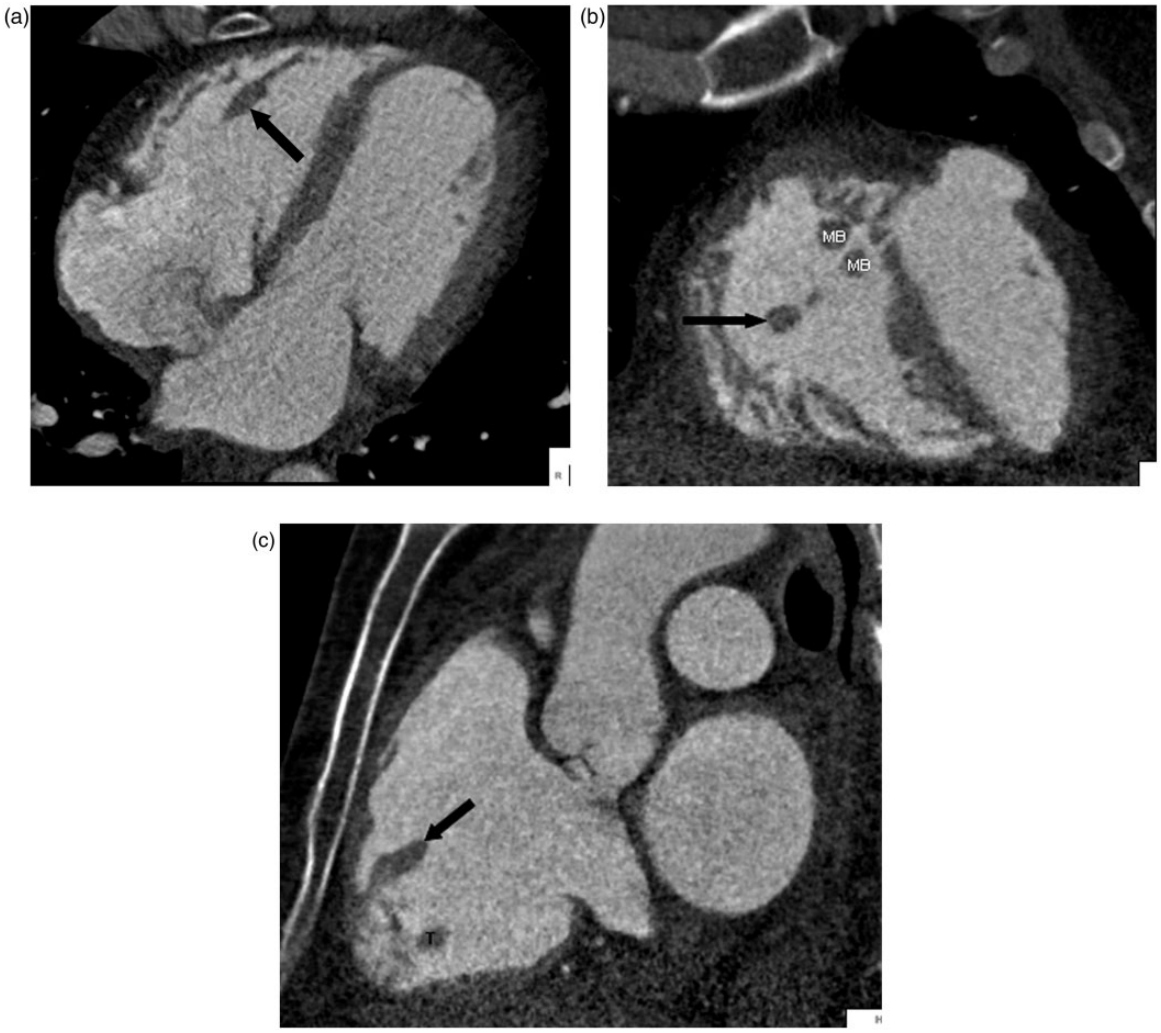


**Fig. 13.** A 62-year-old man with chest tightness. Coronary CTA was performed to evaluate the coronary arteries. Multiplanar imaging shows an ellipsoid shaped anterior papillary muscle in the right ventricle on axial (a), coronal (b), and sagittal (c) planes (black arrows). MB, moderator band; T, trabeculation.

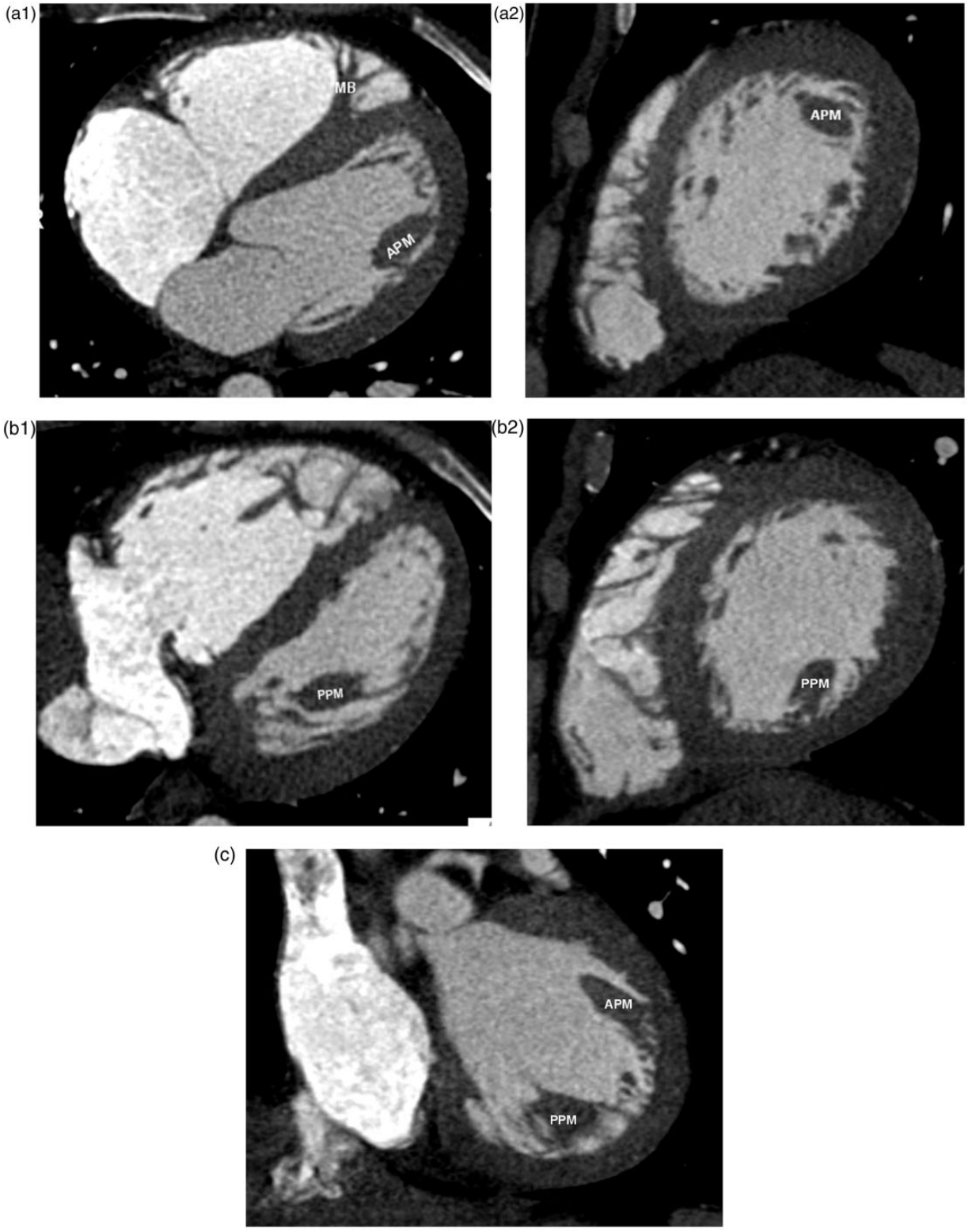


**Fig. 15.** A 40-year-old man with atypical chest pain. Coronary CTA was performed to evaluate the coronary arteries. Multiplanar imaging with axial and sagittal planes of anterior (a1, a2) and posterior papillary muscle (b1, b2) are shown. These are also seen on the coronal image (c). APM, anterior papillary muscle; IVC, inferior vena cava; IVS, interventricular septum; MB, moderator band; MV, mitral valve; PPM, posterior papillary muscle; TV, tricuspid valve.


**Fig. 16.** A 66-year-old woman with atrial fibrillation. A pulmonary vein CT for pre-ablation mapping shows a physiologic apical thinning (arrow). Physiologic thinning of the LV apex is occasionally mistaken as a sequlae of myocardial infarction. Note the prominent posterior papillary muscle (double arrows). RAA, right atrial appendage.


**Fig. 17.** A 53-year-old man with atrial fibrillation. A pulmonary vein CT for pre-ablation mapping pulmonary shows normal thinning of the interventricular septum of the membranous portion (arrow) which can be mistaken as a ventricular septal defect.

considered a normal variant. This normal wall thinning can be mistaken for an old myocardial infarction (Fig. 16). The key to diagnosis is assessment of wall motion during functional evaluation. This can be done if retrospective ECG-gating cardiac CT has been performed or alternatively by echocardiography or cardiac magnetic resonance imaging (MRI) (35).

The interventricular septum consists of a thin membranous portion located immediately beneath the aortic valve and a larger muscular septum (9). The thin membranous septum can simulate a ventricular septal defect (Fig. 17). Lack of visualization of blood flow between two ventricular chambers assures an intact ventricular septum.

## *Sinus of Valsalva*

The sinus of Valsalva of the ascending aorta and main pulmonary artery aligns obliquely to the axial plane. An axial CT slice through the sinus of Valsava will cause sinus of Valsalva to appear distorted and can be mistaken for a sinus of Valsava aneurysm. Sagittal or coronal reformats perpendicular to the aortic and pulmonic valve plane will help to delineate this normal anatomy (36) (Fig. 18a–c).

## *Pericardial recesses*

Pericardial reflection covering the heart and mediastinum can be variable and confusing when containing fluid. These pericardial recesses can mimic mediastinal masses, mediastinal lymphadenopathy, or even pulmonary nodules.

Mediastinal structures, including the heart and great vessels, are covered by the pericardium. The pericardium consists of two layers, the outer fibrous layer and the inner double-layered serous sac. The inner layer is composed of visceral and parietal layers, which become pericardial recesses. The tissues of origin determine the locations of the pericardial recesses, which can be categorized into transverse sinus, oblique sinus and pulmonary venous recesses (37,38).

The transverse sinus is situated posterior to the ascending aorta and main pulmonary artery above the left atrium. It is divided into the superior aortic, inferior aortic, pulmonic, and postcaval recesses depending on its location (Fig. 19). The superior aortic recess is the most prominent and most variable pericardial recess (Figs. 20 and 21). The oblique sinus is located posterior to the left atrium and anterior to the esophagus. It is separated from the transverse sinus by a double layer of pericardium (Fig. 22). As the pulmonary veins join the left atrium, the pericardium incorporates the veins resulting in right and left pulmonary venous recesses (Fig. 23). These recesses are usually small, however, the right pulmonary venous recess is frequently seen.

A summary of normal structures and anatomical variants that can simulate pathology is shown in Tables 1 and 2.


**Fig. 18.** A 56-year-old man with atrial fibrillation. A pulmonary vein CT for pre-ablation mapping shows distortion of the Sinus of Valsalva of the aorta which can simulate the sinus of Valsalva aneurysm (arrows in a). Images perpendicular through the aortic valve (black line in b) will clarify this normal anatomy (c).

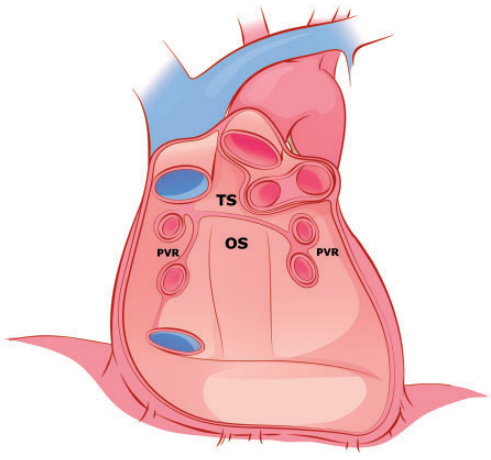


**Fig. 19.** An illustration shows pericardial reflection forming the pericardial recesses from the anterior perspective with the heart removed. OS, oblique sinus; PVR, pulmonic vein recess; TS, transverse sinus. This illustration was modified with permission from: Gray's Anatomy for Students. 2nd edition. Amsterdam: Elsevier, 2010:122–243.

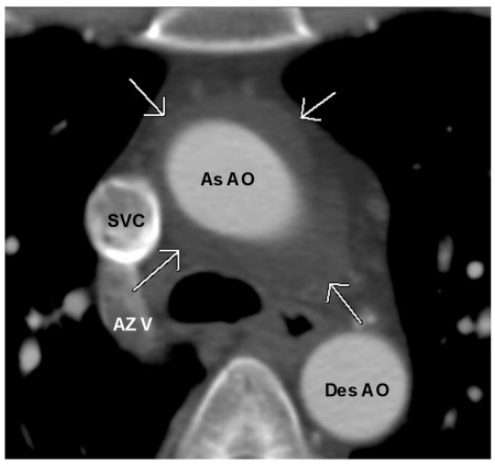


**Fig. 20.** A 41-year-old woman with shortness of breath. A chest CT shows prominent superior aortic recess surrounding the ascending aorta simulating a periaortic hematoma (arrows). As AO, ascending aorta; AZ V, Azygos vein; Des AO, descending aorta.

**Fig. 21.** A 72-year-old man with shortness of breath. An unenhanced chest CT shows the inferior extension of the periaortic recess (arrows), which may be mistaken as subcarinal lymphadenopathy.

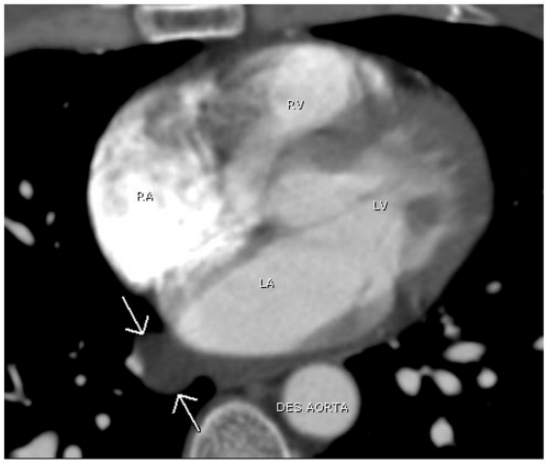


**Fig. 23.** A 43-year-old man with chest pain. A chest CTA performed to rule out PE shows a small outpouching of fluid from the sleeve of right inferior pulmonary vein (arrows). This is the common location for right pulmonary venous recess.


**Fig. 22.** A 65-year-old man with colon cancer. Restaging chest CT shows prominent oblique sinus filling with fluid (arrows). Note fluid filled in the lumen of the minimally thicken esophagus.

**Table 1.** The table summarizes normal structures in the atria that can simulate pathology and how to avid misinterpretations.

| Cardiac chambers | Normal structures | Mimickers | Remarks |
|---|---|---|---|
| Right atrium | Prominent pectinate muscle | Tumor or thrombus | Re-evaluation on MPR |
| | Prominent crista terminalis | Tumor or thrombus | Re-evaluation on MPR |
| | Prominent Eustachian and Thebesian valves | Tumor or thrombus | Re-evaluation on MPR |
| Left atrium | Prominent Ligament of Marshall, Pectinate muscle | Tumor or thrombus | Re-evaluation on MPR |
| | Slugglish flow in left atrial appendage | Thrombus | Repeat delayed scan at 30 s or further investigate with echocardiogram |

(continued)

**Table 1.** Continued.

| Cardiac chambers | Normal structures | Mimickers | Remarks |
|---|---|---|---|
| | Normal thinning of interatrial septum | ASD | Further evaluation with echocardiogram or MRI |
| | Lipomatous hypertrophy of interatrial septum with spared fossa ovalis | ASD | Further evaluation with echocardiogram or MRI |
| | Patent foramen ovale | ASD | Further evaluation with echocardiogram or MRI |

**Table 2.** Normal structures in the ventricles that can mimic diseases and appropriate investigations to prevent misinterpretations.

| Cardiac chambers | Normal structures | Mimickers | Remarks |
|---|---|---|---|
| Right ventricle | Displaced moderator band | Double chamber right ventricle | Further evaluation with echocardiogram or MRI |
| | Prominent moderator band | Tumor or thrombus | Re-evaluation on MPR |
| | Prominent anterior papillary muscle | Tumor or thrombus | Re-evaluation on MPR |
| | Non-specific fat deposition in the RV free wall | Arrhythmogenic Right Ventricular Dysplasia | Further evaluation with echocardiogram or MRI |
| Left ventricle | Prominent posterior papillary muscle | Tumor or thrombus | Re-evaluation on MPR |
| | Normal apical thinning | Prior myocardial infarction | Further evaluation with echocardiogram or MRI |
| | Membranous septum | VSD | Further evaluation with echocardiogram or MRI |

## Conclusion

Awareness of normal cardiac anatomy and anatomic variants will assist cardiothoracic imagers in avoiding misinterpretation of normal findings as pathologic processes.

### Acknowledgements

The authors would like to thank Stacy M Rissing, MD and Shawn Teague, MD for the initial manuscript editing.

### Conflict of interest

None declared.

### Funding

This short report received no specific grant from any funding agency in the public, commercial, or not-for-profit sectors.

### References

1. Moore KL, Persaud TVN. The cardiovascular system. In: Moore KL, Persaud TVN (eds) The Developing Human Clinically Orientated Embryology, 8th edition. Philadelphia, PA: Saunders Elsevier, 2008, pp.285–337.
2. Ginat DT, Fong MW, Tuttle DJ, et al. Cardiac imaging: Part 1. MR pulse sequences, imaging planes, and basic anatomy. Am J Roentgenol 2011;197: 808–815.
3. Broderick LS. Cardiac Anatomy and Pitfalls, Thoracic Imaging 2012, Hyatt Regency Huntington Beach Resort and Spa, Huntington Beach, CA, March 11–14 2012, Meeting.
4. Dick M. Clinical cardiac electrophysiology in the young. In: Dorostkar P (ed.) Development and Structure of the Cardiac Conduction System, 1st edition. New York: Springer Science, 2006, pp.3–15.
5. D'Amato N, Peierfellice O, D'Agostino C. Crista terminalis bridge: a rare variant mimicking right atrial mass. Eur J Echocardiogr 2009;10:444–445.
6. Pharr JR, West MB, Kusumoto FM. Prominent crista terminalis appearing as a right atrial mass on transthoracic echocardiogram. J Am Soc Echocardogr 2002;15: 753–755.
7. Akcay M, Bilen ES, Bilge M, et al. Prominent crista terminalis: As an anatomical structure leading to atrial arrhythmias and mimicking right atrial mass. J Am Soc Echocardiogr 2007;20:e9–e10.
8. Gaudio C, Di Michele S, Cera M, et al. Prominent crista terminalis mimicking a right atrial myxoma: cardiac magnetic resonance aspects. Eur Rev Med Pharmacol Sci 2004; 8:165–168.

9. Halpern EJ. Clinical cardiac CT anatomy and function. In: Halpern AJ, Owen AN (eds) Cardiac Morphology and Function, 2nd edition. New York: Thieme, 2011, pp.174–229.
10. O'Brien JP, Srichai MD, Hecht EM, et al. Anatomy of the heart at multidetector CT: What the radiologist needs to know. Radiographics 2007;27:1569–1582.
11. Meier RA, Hartnell GG. MRI of right atrial pseudomass: is it really a diagnostic problem? J Comput Assist Tomogr 1994;18:398–401.
12. Bear H, Mereles D, Grunig E, et al. Images in echocardiography. Exaggerated pectinate muscles mimicking multiple left atrial appendage thrombi. Eur J Echocardiogr 2001;2:131.
13. Hart RG, Pearce LA, Rothbart RM, et al. Stroke with intermittent atrial fibrillation: Incidence and predictors during aspirin therapy. Stroke Prevention in Atrial Fibrillation Investigators. J Am Coll Cardiol 2000;35: 183–187.
14. Marshall J. On the development of the great anterior veins in man and mammalia: including an account of certain remnants of foetal structure found in the adult, a comparative view of these great veins in the different mammalia, and an analysis of their occasional peculiarities in the human subject. Philos Trans R Soc Lond 1850; 140:133–169.
15. Lin WS, Prakash VS, Tai CT, et al. Pulmonary vein morphology in patients with paroxysmal atrial fibrillation initiated by ectopic beats originating from the pulmonary veins: implications for catheter ablation. Circulation 2000;101:1274–1281.
16. Aliot E, Haissaguerre M, Jackman WM. Catheter ablation of atrial fibrillation. In: Cabrera JA, Farre J, Ho SY, et al. (eds) Anatomy of the Left Atrium Relevant to Atrial Fibrillation, 1st edition. Singapore: Blackwell, 2008, pp.3–30.
17. Gupta S, Plein S, Greenewood JP. The coumadin ridge: an important example of a left atrial pseudotumor demonstrated by cardiovascular magnetic resonance imaging. J Radiol Case Rep 2009;3:1–5.
18. Broderick LS, Conces DJ Jr, Traver RD. CT evaluation of normal interatrial fat thickness. J Comput Assist Tomogr 1996;20:950–953.
19. Burke AP, Litovsky S, Virmani R. Lipomatous hypertrophy of the interatrial septum presenting as a right atrial mass. Am J Pathol 1996;128:630–638.
20. Heyer CM, Kagel T, Lemburg SP, et al. Lipomatous hypertrophy of the interatrial septum: a prospective study of incidence, imaging findings, and clinical symptoms. Chest 2003;124:2068–2074.
21. Wang ZJ, Reddy GP, Gotway MB, et al. Cardiovascular shunts: MR imaging evaluation. Radiographics 2003;23: S181–S194.
22. Casabon L, McLaughlin P, Webb G, et al. Recurrent stroke/TIA in cryptogenic stroke patients with patent foramen ovale. Can J Neurol Sci 2007;34:74–80.
23. Devendra GP, Rane AA, Krasuski RA. Provoked exercise desaturation in patent foramen ovale and impact of percutaneous closure. JACC Cardiovasc Interv 2012;5: 416–419.
24. Goor DA, Lillehei CW. Congenital malformations of the heart. Embryology, anatomy, and operative considerations. In: Goor DA, Lilleher CW (eds) The Anatomy of the Heart, 1st edition. New York: Grune and Stratton, 1975, pp.1–37.
25. Vogel-Claussen J, Shehata ML, Lossnitzer D, et al. Increased right ventricular Septomarginal tribeculation mass is a novel marker for pulmonary hypertension: comparison with ventricular mass index and right ventricular mass. Invest Radiol 2011;46:567–575.
26. Seremi F, Ho SY, Cabrera A, et al. Right ventricular outflow tract imaging with CT and MRI: Part 1, Morphology. Am J Roentgenol 2013;200:W39–W50.
27. Kosinski A, Koztowski D, Nowinski J, et al. Morphological aspects of the septomarginal trabecula in the human heart. Arch Med Sci 2010;6:733–743.
28. Edwards WD. Cardiac anatomy and examination of cardiac specimens. In: Allen HD, Gutgesell HP, Clark EB, et al. (eds) Moss and Adams' Heart Disease in Infants, Children, and Adolescents, Including the Fetus and Young adult, 6th edition. Philadelphia, PA: Lippincott Williams and Wilkins, 2001, pp.1–31.
29. Ravindran P, Victor S. The moderator band. Indian J Thorac Cardiovasc Surg 1982;1:15–21.
30. Wong PC, Sanders SP, Jonas RA, et al. Pulmonary valve moderator band distance and association with development of double chambered right ventricle. Am J Cardiol 1991;68:1681–1686.
31. Bogaert J, Dymarkowski S, Taylor AM. Clinical cardiac MRI. In: Bogaert J, Dymarkowski S (eds) Cardiac Masses, 1st edition. Berlin: Springer-Verlag, 2005, pp.305–351.
32. Guyton AC, Hall JE. Rhythmical excitation of the heart. In: Guyton AC, Hall JE (eds) Textbook of Medical Physiology, 9th edition. Philadelphia, PA: WB Saunders, 1996, pp.121–133.
33. Kim E, Choe YH, Han BK, et al. Right ventricular fat infiltration in asymptomatic subjects: observations from ECG-gated 16 slice multidetector CT. J Comput Assist Tomogr 2007;31:22–28.
34. Keren A, Billingham ME, Popp RL. Echocardiographic recognition and implications of ventricular hypertrophic trabeculations and aberrant bands. Circulation 1984;70: 836–842.
35. Johnson KM, Johnson HE, Dowe DA. Left ventricular apical thinning as normal anatomy. J Comput Assist Tomogr 2009;33:334–337.
36. Broderick LS, Brooks GN, Kuhlamn JE. Anatomic pitfalls of the heart and pericardium. Radiographics 2005; 25:441–453.
37. Troung MT, Erasmas JJ, Gladdish GW, et al. Anatomy of pericardial recesses on multidetector CT: implications for oncologic imaging. Am J Roentgenol 2003;181: 1109–1113.
38. O'Leary SM, Williams PL, Williams MP, et al. Imaging the pericardium: appearances on ECG-gated 64 detector row cardiac computed tomography. Br J Radiol 2010;83: 194–205.